Atmósfera 38, 641-657 (2024)
https://doi.org/10.20937/ATM.53359

Orinoco revisited: Comprehensive analysis of the Orinoco River basin present and future hydroclimate

Alejandro BUILES-JARAMILLO[1]*, Hernán D. SALAS[2], Juliana VALENCIA[1] and Carolina FLORIAN[1]

[1] *Institución Universitaria Colegio Mayor de Antioquia, Facultad de Arquitectura e Ingeniería, Carrera 78 núm. 65-46 Bloque Fundacional piso 2, Medellín, 050034, Antioquia, Colombia.*
[2] *Facultad de Ciencias Exactas y Aplicadas, Instituto Tecnológico Metropolitano, Calle 73 núm. 76A-354, 050034, Medellín, Colombia.*
*Corresponding author; email: luis.builes@colmayor.edu.co

Received: November 21, 2023; Accepted: February 13, 2024

RESUMEN

La cuenca del río Orinoco está clasificada como la tercera más grande de América del Sur y desempeña un papel fundamental en la contribución al volumen de agua del Océano Atlántico. En este estudio proporcionamos una actualización completa del balance hídrico superficial de la cuenca, examinando mediante conjuntos de datos grillados tendencias en la precipitación y la evaporación total. También exploramos los cambios proyectados en la precipitación hasta finales del siglo XXI, enfocándonos al escenario de cambio climático RCP8.5. Para llevar a cabo este estudio utilizamos datos de modelos climáticos regionales del experimento CORDEX-CORE, de donde seleccionamos un ensamble que sobresale en términos de su desempeño en América del Sur y América Central. Cuantificamos la precisión de los datos de referencia en la representación de la dinámica del balance hídrico. Encontramos tendencias crecientes en precipitación y evaporación total en la mayor parte de la cuenca, lo cual aporta al entendimiento del balance hidrológico de la cuenca en el largo plazo. Es notable que tanto la parte Andina como la parte Guayanesa de la cuenca contribuyen por igual al balance hídrico, a pesar de que la segunda abarca sólo el 30 % del área total. Esto resalta la importancia de las subcuencas del escudo guayanés. Respecto a la modelación climática regional, las simulaciones para el dominio CORDEX América del Sur simulan de manera efectiva la precipitación en toda la cuenca, a pesar de cierta subestimación. En cuanto al escenario de cambio climático RCP8.5, los resultados muestran una reducción anual de la precipitación promedio de alrededor del 45 % para toda la cuenca. Estos hallazgos enfatizan la urgencia de adoptar medidas para mitigar posibles efectos adversos en la sostenibilidad hidrológica de la cuenca del río Orinoco, en respuesta a los patrones climáticos en evolución.

ABSTRACT

The Orinoco River basin, ranked as South America's third-largest catchment, is pivotal in contributing to the Atlantic Ocean's water volume. This study provides a comprehensive update on the basin's surface water balance, examining trends using gridded precipitation and total evaporation datasets. We also explore projected changes in precipitation until the end of the 21st century, focusing on the RCP8.5 climate change scenario. To achieve this, we utilize data from regional climate models designed by the CORDEX-CORE experiment, selecting an ensemble that excels in performance across South America and Central America. We estimate the accuracy of reference datasets in capturing water balance dynamics. We identify increasing trends in precipitation and total evaporation across most of the basin, enhancing our understanding of its long-term hydrological balance. Notably, the Andean and Guianese sectors of the basin contribute equally to half of the mean surface runoff, although the latter encompasses only 30% of the total area. This underscores the key role of the Guianese shield sub-basins. In regional climate modeling, despite some underestimation, the model runs for the CORDEX South America domain simulate effectively the precipitation across the basin.

Regarding climate scenarios, our analysis using the RCP8.5 scenario projects an average annual precipitation reduction of around 45% for the entire basin. These findings emphasize the urgency of adopting measures to mitigate potential adverse effects on the Orinoco River basin's hydrological sustainability in response to evolving climate patterns.

Keywords: large scale hydrology, hydroclimatology, climate change, northern South America.

1. Introduction

The Orinoco River basin, spanning approximately 1 million km^2 and boasting a discharge of 3.5×10^4 m^3 s^{-1}, stands as the third-largest basin in South America and ranks similarly in global discharge (López et al., 2012). This vast river basin covers around 70% of Venezuela's continental territory and 30% of Colombia (Fig. 1), exhibiting remarkable ecological diversity due to its strategic location amid the northern Andes, the Caribbean mountain range, the Guianese shield, and the sprawling low relief expanses known as "llanos" in both countries (Warne et al., 2002; Frappart et al., 2012). The Andes and the Guianese Shield, two prominent mountainous regions within the basin, harbor pivotal ecosystems essential for sustaining water availability: the Páramo, primarily situated in the Andes and acting as a highland reservoir (Buytaert et al., 2006), and the Guianese rainforest, instrumental in channeling the water vapor flux from the Atlantic Ocean to the basin and onward to the Amazon basin (Bovolo et al., 2018).

Divided into three main sections, the basin encompasses the Alto Orinoco in the south, characterized by the Ventuari as its primary tributary; the Medio Orinoco, predominantly located within the Colombian Orinoco region and featuring tributaries like Inirida, Vichada, Guaviare, Meta, and Arauca; and finally, the Bajo Orinoco near the delta, where the Caroni and Caura emerge as the most significant tributaries (Silva, 2005; Frappart et al., 2012). Additionally, the Orinoco River basin shares a border with the Amazon River basin, with

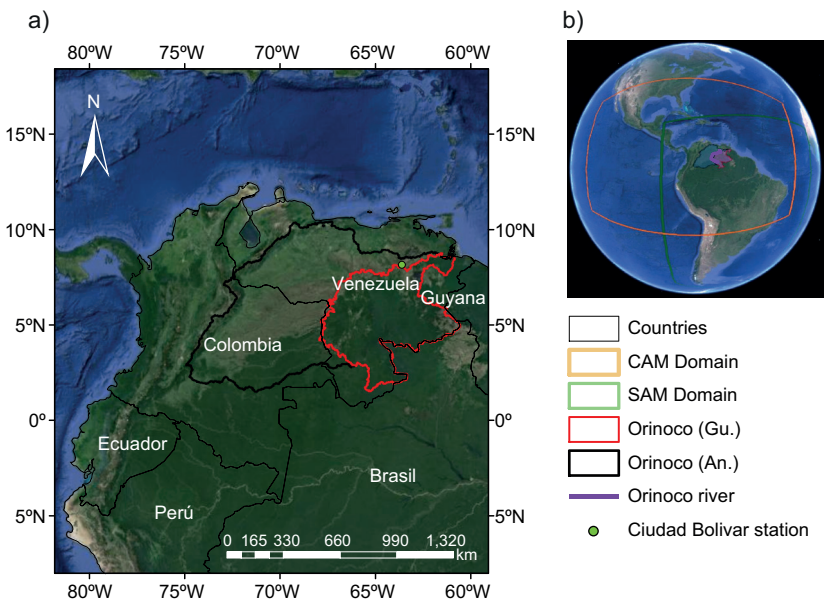

Fig. 1. (a) Study region: the Orinoco River basin on northern South America (black: Andean slope; red: Guiana Shield). (b) Context of the CORDEX-CORE domains for South and Central America (CAM/SAM)

both basins acting as crucial sources of Andean sediments and dissolved rare elements feeding into the Atlantic Ocean (Meade, 2008; Mora et al., 2020).

The precipitation patterns in the Orinoco River basin showcase a distinctive unimodal annual cycle, marked by a dry season during December-January-February (DJF) and a contrasting wet season spanning June-July-August (JJA) (Labar et al., 2005; Urrea et al., 2019). Notably, the hydroclimatology during DJF is predominantly influenced by the Orinoco Low-Level Jet (OLLJ), which contributes to the dry season through low-level wind divergences (Labar et al., 2005; Jiménez-Sánchez et al., 2019; Builes-Jaramillo et al., 2022; Martínez et al., 2022). Conversely, the Cross-Equatorial Flow (CEF) plays a pivotal role during JJA, transporting moisture from the Amazon River basin to the Orinoco River basin and thereby causing the wet season (Builes-Jaramillo et al., 2022; Wang and Fu, 2002). Despite its crucial role in the hydroclimate of northern South America, the Orinoco River has received limited attention in recent decades, with scarce efforts directed towards estimating its long-term water balance (Silva, 2005).

While studies analyzing climate change trends within Venezuela and Colombia exist (Falloon and Betts, 2006; Brêda et al., 2020, Arias et al., 2021; Miranda et al., 2023; Viloria et al., 2023), a comprehensive analysis of historical trends in hydrological variables specifically emphasizing the impact of the Andes and Guiana Shield mountain ranges on the basin's surface runoff, and integrating downscaled information is noticeably absent. Hence, regional climate models (RCMs) offer an alternative to global climate models (GCMs), as RCMs can simulate higher spatial resolutions, providing more intricate representations of climatic features for smaller areas. Notably, the Coordinated Regional Downscaling Experiment (CORDEX) serves as a key resource for this endeavor. Within CORDEX, the Coordinated Output for Regional Evaluations (CORDEX-CORE) initiative aims to provide consistent projections across several planetary domains, using a core set of RCMs driven by common GCMs with standardized simulation protocols (Remedio et al., 2019; Giorgi et al., 2021). For the CORDEX-CORE experiment, two RCMs, namely RegCM4 (Giorgi et al., 2012) and REMO (Pietikäinen et al., 2018), have been implemented.

CORDEX-CORE has implemented several domains around the world, particularly for northern South America. The South America (SAM) and Central America (CAM) domains are useful for regional climate change assessments. According to the literature, RCMs in the CAM domain have a better performance in reproducing air-sea interactions, leading to better representation of key circulation patterns such as the Intertropical Convergence Zone (ITCZ) and reduced precipitation over land and oceans (Remedio et al., 2019; Cavazos et al., 2020), as well as in coastal regions. In contrast, SAM domain simulations show less precision due to the Andes high altitudes (Jacob et al., 2012; Ashfaq et al., 2021; Reboita et al., 2021).

Recognizing the potential for an in-depth analysis of the Orinoco River basin, we studied the historical long-term surface water balance in the basin addressing the following questions: (*a*) how do the estimates of long-term basin balance differ when utilizing models and remote sensing ensembled with reanalysis datasets?; (*b*) are there discernible trends in hydrological variables across the Orinoco basin for the historical period of 1981-2014?; (*c*) which mountain range exerts a greater influence on surface runoff in the basin, the Andes or the Guianese shield?; (*d*) do the CORDEX-CORE RCMs effectively represent the surface water balance of the Orinoco River basin?; and (*e*) among the RCM ensembles from the CORDEX-CORE experiment, which demonstrate optimal performance in representing precipitation patterns?

Furthermore, in anticipation of future climate scenarios for the basin, the study aims to explore: (*a*) how do precipitation trends unfold under the future climate change scenario RCP8.5 during the period 2060-2100; and (*b*) if there is a notable alteration in long-term mean precipitation between the future climate change scenario RCP8.5 for 2060-2100 and the historical period 1981-2014.

This work is organized as follows: section 2 outlines the datasets and methods adopted for the surface water balance analysis, model selection, and bias correction; section 3 presents the results and ensuing discussions, and section 4 concludes the study and presents future work.

2. Datasets and methods

The present study is divided into three main stages:

a) Analysis of the historical long-term water balance and historical trends in the variables of the Orinoco River basin with state-of-the-art datasets.
b) Analysis of the performance of historical scenarios from the CORDEX-CORE RCMS.
c) Analysis of the projected changes in the hydrological cycle over the Orinoco River basin.

2.1 Reference datasets

As a reference, we use monthly datasets gridded for precipitation (P) and total evaporation (E) at 0.25º × 0.25º for the common period 1981-2014. For precipitation, we use three datasets: (*i*) atmospheric reanalysis ERA5 (Hersbach et al., 2020), (*ii*) Global Precipitation Climatology Centre Full Data Reanalysis (GPCC) v. 7 (Schneider et al., 2014), and (*iii*) Climate Hazards Group InfraRed Precipitation with Station (CHIRPS) (Funk et al., 2015). For total evaporation, we use three datasets: (*i*) ERA5, (*ii*) Global Evaporation Amsterdam Model (GLEAM) (Martens et al., 2017), and (*iii*) Global Land Data Assimilation System (GLDAS) (Rodell et al., 2004). For the streamflow of the Orinoco River basin, we use the time series at the Ciudad Bolívar gauge for 2003-2010, which is obtained from the So-Hybam project website (HyBAm, 2023).

2.2 CORDEX-CORE

The CORDEX-CORE simulation framework includes the implementation of two RCMs driven by at least three GCMs in each domain. The RegCM4 and REMO models are the RCMs available for the SAM and CAM domains, while Table I lists the GCMs downscaled by each RCM. The study area is located in the northernmost SAM domain, while for the CAM domain it is located in a more central position, which implies an overlapping position between the domains (Fig. 1). Although different basins are situated between these domains, there is a lack of performance analysis between the SAM and CAM runs. Each model run was gridded to a 0.25º × 0.25º common grid, using bilinear interpolation (Accadia et al., 2003) for the ease of comparison. In total, we have a dataset of 12 downscaled model runs, six for each domain (CAM/SAM). We calculated multi-member ensembles as the mean value of reference datasets (Ens-Ref), and each RCM implementation in each domain: (*i*) RegCM-SAM, (*ii*) RegCM-CAM, (*iii*) REMO-SAM, and (*iv*) REMO-CAM. Hence, every ensemble is composed of three members. Multi-member ensembles are useful to lower the model uncertainties of each RCM implementation at a seasonal time scale (Hagedorn et al., 2005).

2.3 Present long-term surface water balance and trends

The long-term surface water balance was quantified using Eq. [1], where P is the mean precipitation in the basin and E is the mean total evaporation (Peixoto and Oort, 1993; Marengo, 2005; Zhang et al., 2008), acknowledging that this approach is the simplest one and that its selection is based on the size of the basin ($> 500 \times 103$ km^2) and the length of observations (> 30 years). Therefore, this approach is useful under the assumption that for large areas, subterranean runoff is negligible as the storage rate is for long periods. Once we know the performance of the reference datasets, we achieve two goals: (*i*) to update the long-term balance of the Orinoco River basin using state-of-the-art datasets, and (*ii*) to produce an

Table I. CORDEX-CORE datasets: HadGEM2-ES (Martin et al., 2011), MPI-ESM-LR (Giorgetta et al., 2013), NorESM1-M (Bentsen et al., 2013), and GFDL-ESM2M (Dunne et al., 2012).

Domain	SAM		CAM	
RCM	RegCM4	REMO	RegCM4	REMO
GCM1	HadGEM2-ES	HadGEM2-ES	HadGEM2-ES	HadGEM2-ES
GCM2	MPI-ESM-LR	MPI-ESM-LR	MPI-ESM-LR	MPI-ESM-LR
GCM3	NorESM1-M	NorESM1-M	GFDL-ESM2M	NorESM1-M

ensemble for precipitation to be used as a reference for comparison analysis with the historical runs of the RCMs. The runoff (R) was computed as $R = Q/A$ (Builes-Jaramillo and Poveda, 2018), where Q represents the long-term monthly mean streamflow and A is the area of the river basin (860 000 km^2 at the Ciudad Bolivar gauge). Then, the estimations of Q using RCMs are compared with the observed long-term mean streamflow in the Ciudad Bolívar gauge and previous works (Silva, 2005).

$$P - E = R \tag{1}$$

We computed Kendall's non-parametric test (Kendall, 1975) for a monotonic trend using the Theil-Sen method (Sen, 1968) to estimate the slope in each grid point for P and E.

2.4 Andes-Guiana runoff

The long-term surface runoff (R) is computed as the difference of the long-term mean of P and E for the total area of the river basin, as well as for the river basin divided into two sections (Fig. 1): (*a*) the Andean section of the basin that includes sub-basins located in the eastern Andean mountain range territory (609 652 km^2); and (*b*) the Guiana section, which includes sub-basins located in the Guianese shield territory (250 347 km^2). The separation of the basin into two portions helps to identify if there is an imbalance in terms of the water runoff that feeds the river streamflow.

2.5 Model performance assessment method

Using the ERA5, GPCC, and CHIRPS precipitation datasets, we compute an ensemble that serves as a reference. Then, we calculate the mean spatial correlation between the reference ensemble and the CORDEX-CORE historical simulations to assess the models' performance. Moreover, we compute the Arcsin M (Eq. [2]) skill metric (Watterson et al., 2014; Solman and Blázquez, 2019) for each RCM/domain ensemble.

$$M = \frac{2}{\pi} arcsin\left(1 - \frac{MSE}{V_X + V_Y + (G_X - G_Y)^2}\right) \times 100 \tag{2}$$

where MSE is the mean square error between the modeled and observation fields, Y and X, respectively. Furthermore, V is the variance and G is the mean. The final factor provides a skill score that has a maximum possible value of 1000 (for $MSE = 0$). With the M performance metric and spatial correlations, we will be able to select the models with best performance in the region.

2.6 Bias correction method

Once we found the CORDEX-CORE model ensemble with the best performance, we chose it in order to perform the bias correction. For that RCM ensemble, we downloaded the simulations for the RCP8.5 scenario for the period 2060-2100, regionalized by the CORDEX-CORE experiment. These simulations are bias-corrected according to the delta (Eq. [3]) and linear scaling (Eq. [4]) methods as proposed by Teutschbein and Seibert (2012). We selected these two methods for the bias correction because they are robust for long-term monthly analysis (Brêda et al., 2020), as the one in the present study.

$$P_{BC} = P_r\left(\frac{\mu_m(P_f)}{\mu_m(P_{sp})}\right) \tag{3}$$

$$P_{BC} = P_f\left(\frac{\mu_m(P_r)}{\mu_m(P_{sp})}\right) \tag{4}$$

where PBC is the monthly bias corrected precipitation, P_r is the observed precipitation during the historical period, P_f is the simulated precipitation for the future period, P_{sp} the simulated precipitation for the historical period, and $\mu_m(\cdot)$the mean monthly value for the simulation or observation periods. It is worth noting that the delta method is applied to correct the bias in the observed dataset, whereas the linear scaling method is applied to correct the bias in the simulated future.

With the bias-corrected datasets, we compute annual cycles and spatial biases between the RCP8.5 projections and reference dataset ensembles. In this way, we are able to assess the seasons when future projections show changes in water availability and where there will be greater perturbations in the Orinoco River basin.

3. Results

3.1 Long-term surface water balance and trends

Figure 2 shows the mean fields and trends of P and E from the reference datasets ensembles for the Orinoco River basin. According to the reference

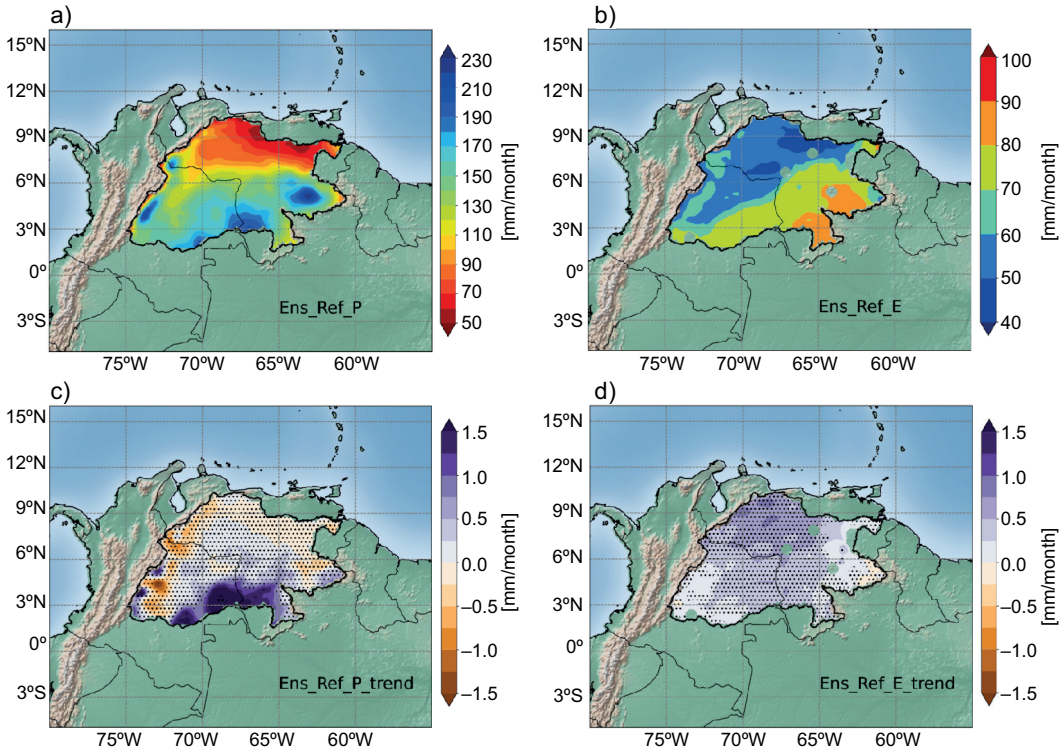

Fig. 2. Mean fields from the reference datasets ensemble during the period 1981-2014 for (a) precipitation (*P*) and (b) total evaporation (*E*). Trend fields from the reference datasets ensemble during the period 1981-2014 for (c) precipitation (*P*) and (d) total evaporation (*E*). Dots in trend fields depict the pixels with a significant trend according to the Theil-Sen method and the Kendall test.

datasets ensemble, the lower values of mean *P* in the basin are located in central Venezuela, with values from 50 to 80 mm month^{-1}, whereas the highest values of mean *P* in the eastern flanks of the Andes and the Guianese shield had values from 200 to 230 mm month^{-1}, which highlight the importance of the two mountain ranges for precipitation in the Orinoco River basin (Fig. 2a). In terms of trends (Fig. 2c), our results suggest that *P* decreases in the north and northeastern basin territory (–0.5 mm decade^{-1}) and eastern flanks of the Andes (–1.0 to –1.5 mm decade^{-1}), while *P* shows positive trends in the south of the basin (1.0-2.0 mm decade^{-1}).

Regarding *E*, the reference datasets show the highest values in the Guianese shield of the basin (80-90 mm month^{-1}) and the lower values in the Llanos region between Colombia and Venezuela, the eastern flanks of the Andes, and the coastal mountain range in northern Venezuela (values of 40-60 mm month^{-1}) (Fig. 2b). Reference datasets for *E* show a higher increasing trend in the north of the basin (1.0 mm decade^{-1}), whereas the easternmost portion of the basin exhibits a slight decreasing trend (–0.5 mm month^{-1}) (Fig. 3d). It is worth noting that the north (southeast) of the basin, where there are decreasing (increasing) trends in *P*, is the same region with increasing (decreasing) trends in *E*.

The annual cycles of both *P* and *E* are shown in Figure 3. All datasets represent the unimodal annual cycle for *P* in the basin, with the highest values between June-July (around 350 mm month^{-1}) and lowest values in January (50 mm month^{-1}) (Fig. 3a). In terms of *E*, data sources show less evaporation from January to May (in the range 75-90 mm month^{-1}) than from June to September (110-120 mm month^{-1}) (Fig. 3b). An analogous analysis was carried out considering the river basin in their Andean and Guianese territories separately.

In Figure 3c, d it is evident that the annual cycles of *P* are similar in shape (unimodal, peaking around

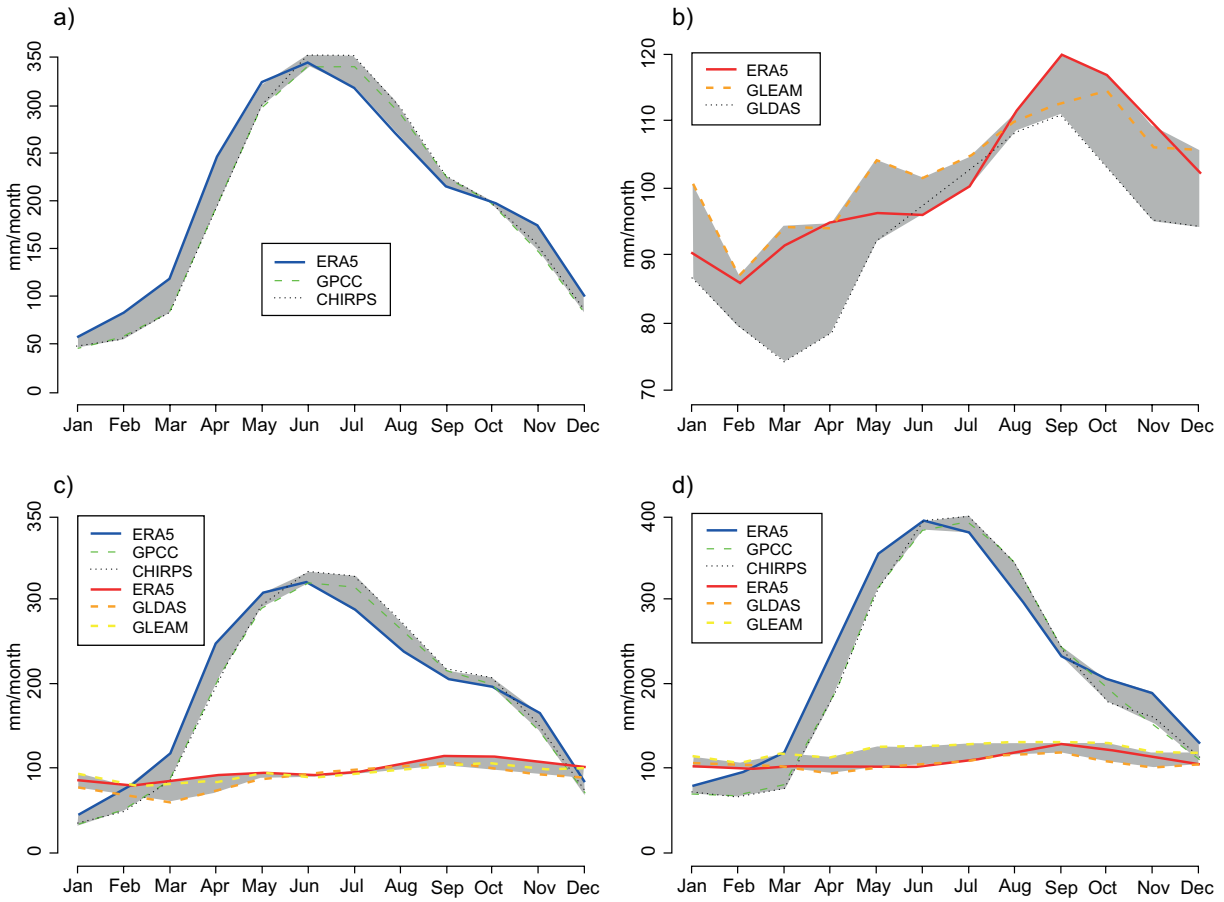

Fig. 3. Annual cycles of reference datasets over the Orinoco basin (in mm month^{-1}). (a) Precipitation, (b) total evaporation, (c) precipitation and total evaporation over the Andean portion of the Orinoco basin, and (d) precipitation and total evaporation over the Guiana portion of the Orinoco basin. The grey area shows the dataset's variability.

midyear); however, the Andean portion of the basin shows a lower peak (300 mm month^{-1}) than the one exhibited by the Guianese portion of the basin (400 mm month^{-1}). In January, we found that P is also lower in the Andean portion of the basin (50 mm month^{-1}) than in the Guianese portion (100 mm month^{-1}). We present a schematic summary of the results for the entire basin and for the two portions in Figure 4, including the accumulated monthly values computed from the ensemble of reference datasets for P and E. In general, the Andean and Guianese portions of the basin generate the same amount of runoff, with differences lower than 1%. This shows the importance of both mountainous regions for the hydrological stability of the basin.

We computed the long-term streamflow for the reference datasets ensembles of P and E (Table II). Our results suggest that the differences between streamflow observations at the Ciudad Bolívar gauge and those by Silva (2005) are negligible (–4.8% to –6.1%). This result shows that by means of model ensembles, it is possible to obtain a robust representation of the long-term water balance. However, previous analyses for total evaporation and evapotranspiration products over South America have proven to possess significant shortcomings in the simulation of this variable (Sörensson and Ruscica, 2018; Builes-Jaramillo and Pántano, 2021); therefore, a good long-term closure of the surface water balance is not enough to decide on the performance

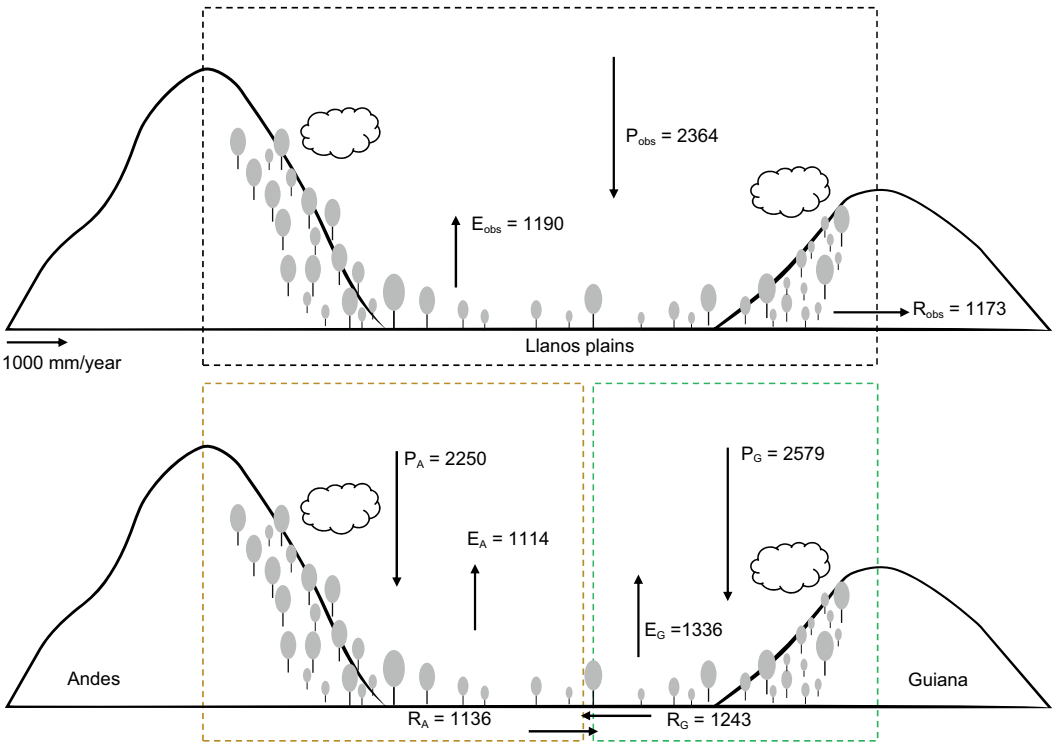

Fig. 4. Schematic representation of the Orinoco River basin considering its Andean and Guianese portions. Top panel: water balance computation for all the Orinoco River basin. Bottom panel; water balance for the Andean (yellow dashed box) and Guianese (green dashed box) portions separately. *P*, *E* and *R* depict the long-term accumulated values of the components in the water balance equation (in mm year^{-1}).

Table II. Runoff computed from the long-term water balance equation for the entire basin and the two portions.

P-E/Q (dataset)	*P-E* (mm/year)	*Q* (m3 /s)	Difference *Q* (%)
P-E (P_R-E_R)	1,173	31,996	
Q (So-Hybam)	1,249	34,069	-6.1
P-E/Q Silva León, (2005)	1,145	33,600	-4.8

P_R: ensemble value computed from the ERA5, CHIRPS, and GPCC datasets; E_R: ensemble value computed from the ERA5, GLDAS, and GLEAM datasets.

of the regional models. Hence, hereafter we assess the model selection by using only the *P* ensemble.

3.2 Model selection

We computed the REMO and RegCM RCMs ensembles in the CAM and SAM CORDEX-CORE domains. Thus, we have ensembles from: (*i*) RegCM-SAM, (*ii*) RegCM-CAM, (*iii*) REMO-SAM, and (*iv*) REMO-CAM. Figure 5a shows the annual cycle of *P* for the reference ensemble (CHIRPS, GPCC, and ERA5) and the ensemble of the RCMs models. On one hand, the best performance for the annual cycle of *P* simulated by models is over the SAM domain (red lines), although there is a mean underestimation

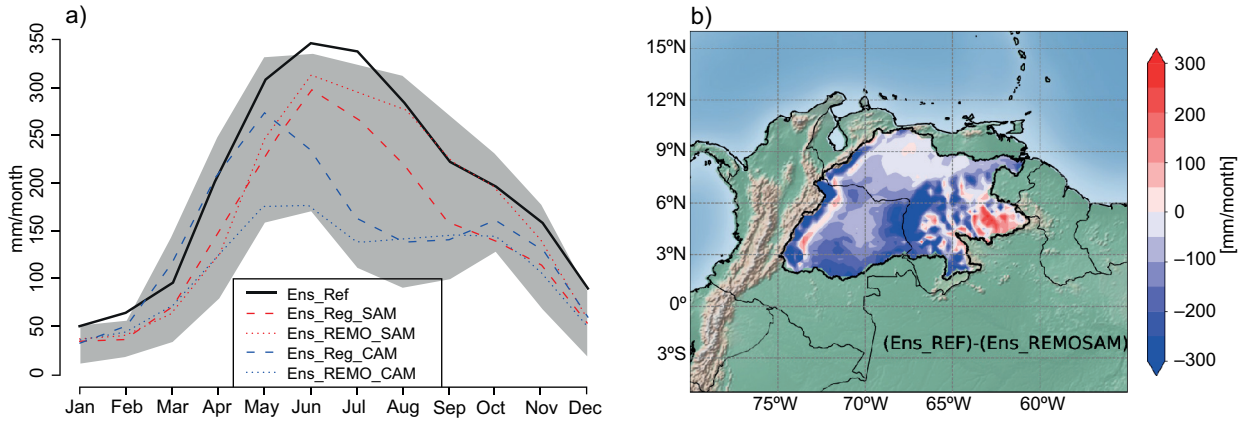

Fig. 5. (a) Annual cycles of precipitation (in mm month^{-1}) for the ensembles of reference datasets and available models from CORDEX-CORE over the Orinoco River basin. The grey area shows the ensembles inter member variability. (b) Precipitation bias field with respect to the reference dataset from the REMO-SAM ensemble for the historical period 1981-2014.

of *P* for the reference period of the SAM ensembles of around 25%. On the other hand, the ensembles computed from the models over the CAM domain (blue lines) fail to simulate the annual cycle of P in terms of its magnitude and variability, with an underestimation of nearly 40% in the wet season (April-September). In the bias field of the best RCM representation of the annual cycle (REMO-SAM ensemble) (Fig. 5b), we can observe regions where *P* is overestimated (100-300 mm month^{-1}) by the RCM ensemble, contrary to the annual cycles shown in Figure 5a, which exhibit an underestimation by the REMO-SAM ensemble during the entire year.

The biases are computed as the ensemble of reference datasets minus each one of the model ensembles (Ens-Rref). Figure 6a shows that models underestimate precipitation (positive values) elsewhere than the eastern flank of the Andes mountain range and the Guianese shield (negative values). The highest underestimation (overestimation) of *P* is given by the REMO-CAM (REMO-SAM) ensemble. Furthermore, Figure 6b shows the spatial Pearson's correlation between reference and RCM ensembles over the river basin. In general, the higher correlations are found in the Llanos region between Colombia and Venezuela, while the lower correlations are located in the Andean flanks, the outflow zone (delta), and the southern portion of the basin.

Figure 6 evidences a lower bias and higher spatial correlations for the RegCM model (RegCM-CAM-RegCM-SAM). Table III includes the results for the Arcsin M and the mean spatial correlation r for the entire basin. M exhibits higher values (closer to 1000) for the REMO model in both CAM and SAM domains, whereas r shows higher values for the RegCM and REMO models in the CAM and SAM domains, respectively. Moreover, we computed the M and r metrics for the wet and dry seasons, April-September and October-March, respectively, to assess the skill of RCMs to represent the periods of high and low precipitation throughout the year. During the dry season, we found a better performance for the ensembles over the CAM domain. After an overall model ensemble analysis, the best performance skill during the wet season was found for the REMO model ensembles regardless of the domain. Therefore, we selected the REMO-SAM to assess the future projections of *P* according to the RCP8.5 scenario included in the CORDEX-CORE experiment for its lower underestimation of the annual cycle variability (19%; Fig. 5a) and higher values of M and r (Table II). Hence, previous results suggest that the REMO-SAM model presents a better performance simulating *P* in the basin.

3.3 Future precipitation over the Orinoco River basin

We used the REMO-SAM ensemble to assess changes in precipitation according to the RCP8.5 scenario. Figure 7a shows that, in terms of annual variability

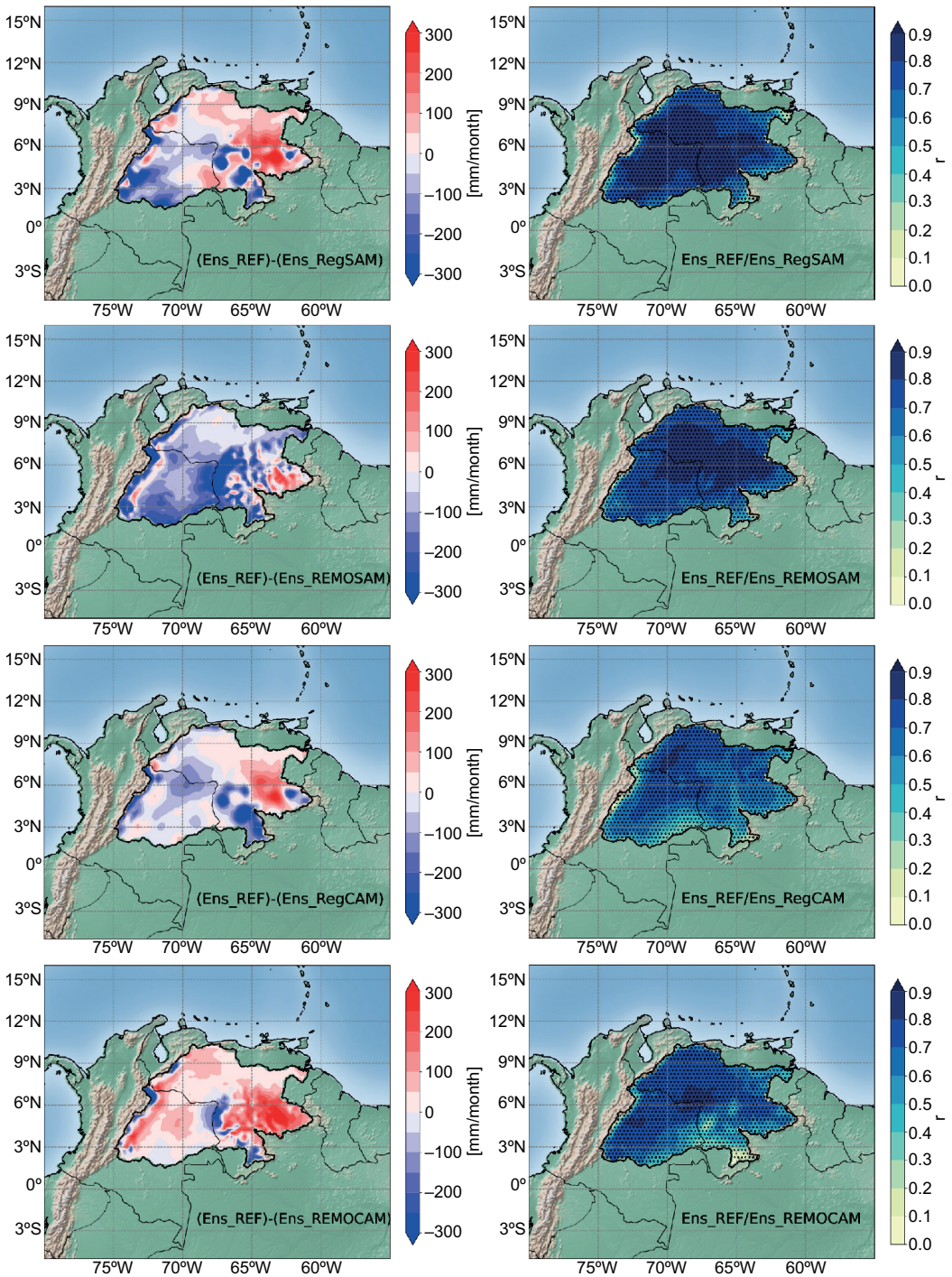

Fig. 6. Left column: fields of precipitation bias for each one of the RCM/domain ensembles. Right column: correlation between the reference datasets ensemble and each one of the RCM/domain ensembles. Correlations are for the monthly time series in each domain pixel. Dots in the correlation fields denote a 95% significance.

Table III. Arcsin Mielke M and spatial correlation r for all model ensembles during the study period 1981-2014 and for the wet and dry seasons over the basin.

	Long-term estimation		Dry season		Wet season	
Ensemble	M	r	M_d	r_d	M_w	r_w
RegCM-CAM	561	0.76	770	0.66	809	0.20
REMO-CAM	727	0.66	781	0.63	829	0.23
RegCM-SAM	697	0.64	608	0.62	756	0.48
REMO-SAM	718	0.75	752	0.67	828	0.41

M d/w: Arsin Mielke M during the dry (wet) season; r d/w: spatial correlation during the dry (wet) season.

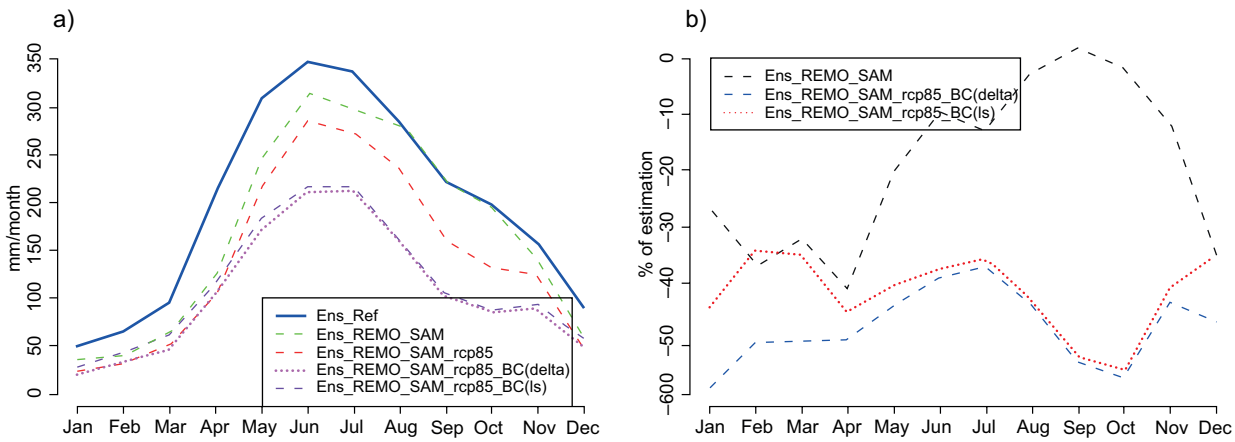

Fig. 7. (a) Annual cycles of Precipitation in mm month^{-1} from the ensemble of reference datasets and ensembles of the REMO Regional Model for the SAM region (historical, future, and bias-corrected). (b) Estimation of monthly precipitation as a percentage of the mean precipitation observed in the reference datasets.

representation, annual precipitation cycles for the future period 2060-2100 without bias correction (red line) are similar to the one found for the historical period in the SAM domain (green line), with a reduction in the simulated precipitation for all the year. After bias correction of the RCP8.5 simulations (Fig. 7a, purple lines), we found reductions in the magnitude of monthly *P* ranging from 40 to 60% regarding the precipitation quantified for the historical period. According to Brêda et al. (2020), the mean reductions in precipitation for northern South America and the Orinoco basin are higher than 35% based on CMIP5 simulations for the RCP8.5 scenario. In particular, for the REMO-SAM ensemble, the percentage of change is computed as the bias-corrected precipitation minus the reference precipitation data set divided by the reference (Fig. 7b). The percent of change in the basin is higher during September-October, at the onset of the dry season. The mean underestimation of precipitation for the future period is 42% for the delta method bias-corrected ensemble and 47% for the linear scaling bias-corrected ensemble.

Figure 8 presents the precipitation bias between the reference and future periods for the REMO-SAM ensembles, using bias correction. Figure 8 shows that for the RCP8.5 scenario, REMO tends to underestimate precipitation in the mountainous regions of the Andes and the Guianese Shield, whereas it is overestimated in parts of the Llanos lowlands and south of the Guianese shield. Figure 8a, b shows that both bias-corrected ensembles agree for the future period simulated by the REMO-SAM ensemble (RCP8.5 scenario). The higher reductions of precipitation are located in the Guianese (around

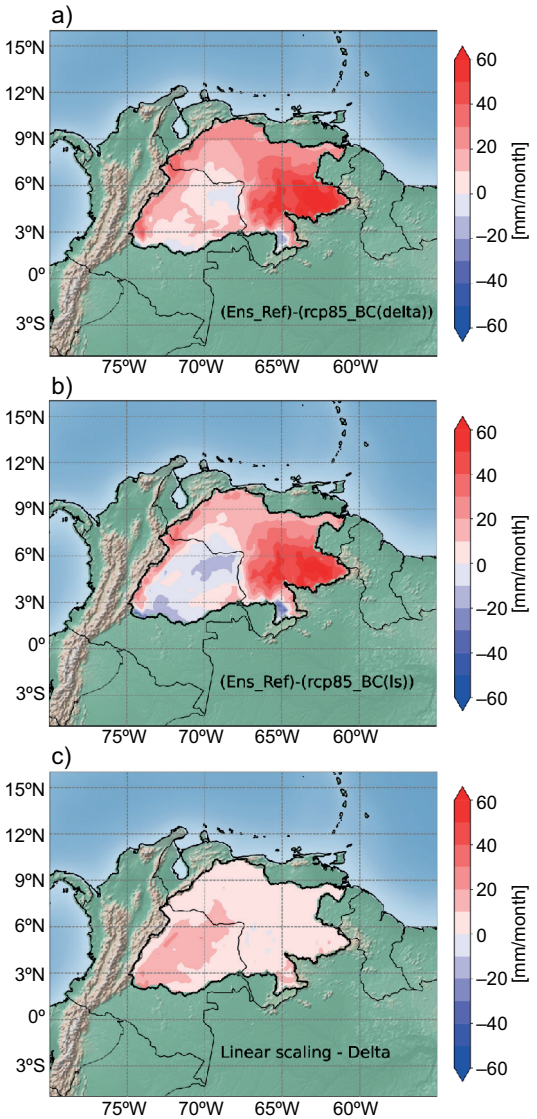

Fig. 8. Bias fields of precipitation with respect to the reference dataset from: (a) bias-corrected REMO-SAM ensemble for the rcp85 scenario with the delta method; (b) bias-corrected REMO-SAM ensemble for the rcp85 scenario with the linear scaling method, and (c) bias between mean fields of bias-corrected simulations (linear scaling-delta).

300 mm month^{-1}) portion and in the eastern flanks of the Andes (around 150 mm month^{-1}). Moreover, according to the REMO-SAM ensembles, our results suggest that precipitation increases in the Llanos corridor between Colombia and Venezuela (around 50 mm month^{-1}). In Figure 8c, we compare the spatial differences between the two bias-correction methods; the higher differences are found in the Llanos and southern Guianese shield.

4. Conclusions and future work

We investigated the present and future hydro-climatology of the Orinoco River basin, one of the most relevant basins in South America but, paradoxically, one of the least studied in terms of future hydro-climatology scenarios. We updated the surface water balance of the basin with several state-of-the-art gridded datasets and estimated long-term trends for these variables. Also, we analyzed the importance of the Andean and Guianese portions of the basin in terms of water production. In this sense, we found that the regions with negative precipitation trends are, in fact, those with positive total evaporation trends for the long term and that each mentioned mountainous portion of the basin constitutes approximately half of the total runoff, which highlights the importance of the mountain ranges for the water production and hydrological stability of the basin. Our results provide new insights into the relevance of the Guianese portion, which is only 30% of the total area of the basin but accounts for 50% of the surface runoff, and also gives further evidence of the importance of the Andes for the stability of the two biggest basins of northern South America, the Amazon (Builes-Jaramillo and Poveda, 2018) and the Orinoco River basin.

For the historical period 1981-2014, we found that the reference datasets reproduce the general features of the annual cycle for precipitation. However, total evaporation exhibits shortcomings and discrepancies that have been previously mentioned for diverse datasets in South America (Sörensson and Ruscica, 2018; Builes-Jaramillo and Pántano, 2021). Furthermore, P and E exhibit increasing trends, which provide evidence of perturbations in the hydrological cycle of the basin, a hydroclimate feature that has also been reported for the Amazon River basin (Gloor et al., 2013; Barichivich et al., 2018). Notwithstanding, the reference datasets ensemble adequately represents the runoff and mean streamflow of the basin with errors below 7%. Thus, recent developments in remote sensing become an important tool for providing hydroclimatological information for the basin scale; nevertheless, this approach may not be suitable for

smaller basins or finer timescales, as observational datasets are needed for bias correction or validation.

We assessed the performance of the regional climate CORDEX-CORE models over the basin for the Central America (CAM) and South America (SAM) domains. Our results suggest that precipitation is underestimated over the SAM domain the whole year, although it is fairly represented, while for the CAM domain precipitation is underestimated during the wet season at around 40%. In general, all ensembles exhibit shortcomings in the representation of precipitation over the Andean slopes and the Guianese shield. We selected the REMO-SAM ensemble because of its better skill according to the Arcsin M metric, spatial correlations, and annual cycle representation. We are aware that selecting one model as the correct one may result in false positives, which is why we have used several metrics to evaluate the performance. Another approach could be to do the ensemble with all the models available after discarding those more evidently wrong.

For the future RCP8.5 scenario 2060-2100, we found, after bias correction of the datasets, that precipitation reduces between 42 and 47% for the REMO-SAM ensemble during the May to October period, which can be interpreted as a reduction of the rainy season or as an abrupt change in the magnitude of precipitation in the period of transition between wet and dry season. This result agrees with the projections of reductions higher than 35% reported by Brêda et al. (2020) for northern South America based on CMIP5 GCMs. Those reductions of almost half of the precipitation around the year in the region, also reported by Arias et al. (2023), added to the ongoing trend of deforestation in the Guianese rainforest, could enhance the severity of droughts in the basin (Sorí et al., 2023) and accelerate the savannisation of the region (Valencia et al., 2023). These alterations could lead to a reduction of the water vapor flux from the Atlantic Ocean towards the Amazon basin (Nieto et al., 2008; Bovolo et al., 2018) that transit through the Orinoco River basin; a reduction of the outflow of precipitation from the Orinoco basin towards Northern South America via moisture recycling (Hoyos et al., 2018; Escobar et al., 2022); extreme precipitation events (Martínez et al., 2023), or even the role of Central America as an evaporative source (Durán-Quesada et al., 2017).

Our results of a decreased mean precipitation in the Orinoco River basin, based on CORDEX-CORE (CMIP5), agrees with the AR6 regional analysis for northern South America, which reports medium confidence on the decrease of mean precipitation for the tropical region (Sun et al., 2019; IPCC, 2021a, b). Given this context, efforts in the region derived from the AR7 assessment report could be oriented to improve the representation of the land/atmosphere feedback to better comprehend the impacts on water availability that sustains the basin's fragile ecosystems. As part of future work, we propose conducting a comprehensive, long-term evaluation by comparing observational datasets, GCMs from the CMIP6 run, and the newly regionalized generation of GCMs across basins of diverse sizes. This analysis will encompass both historical and future scenarios, enabling us to establish a confidence level to identify suitable models for accurately representing the hydroclimatology of each basin based on its specific area.

Acknowledgments

The authors thank the research groups and institutions that provided complete access to the model results through the Earth System Grid Federation (ESFG) nodes (https://esgf.llnl.gov/), to the Copernicus data store where the ERA5 reanalysis is stored (https://cds.climate.copernicus.eu/), to the NOAA Physical Sciences Laboratory where the GPCC dataset is stored (https://psl.noaa.gov/data/gridded/data.gpcc.html), to the UC Santa Barbara Climate Hazards Center where the CHIRPS dataset is stored (https://www.chc.ucsb.edu/data/chirps), to the Gleam model team (https://www.gleam.eu/), and to the NASA Land Data Assimilation System where the GLDAS dataset is available (https://ldas.gsfc.nasa.gov/ldas/land-data-assimilation-system). The authors give a special acknowledgment to Valeria Fajardo-Castaño for the Andean-Guianese profiles illustration (Fig. 4).

References

Accadia C, Mariani S, Casaioli M, Lavagnini A, Speranza A. 2003. Sensitivity of precipitation forecast skill scores to bilinear interpolation and a simple

nearest-neighbor average method on high-resolution verification grids. Weather and Forecasting 18: 918-932. https://doi.org/10.1175/1520-0434(2003)018<0918:SOPFSS>2.0.CO;2

Arias PA, Ortega G, Villegas LD, Martínez JA. 2021. Colombian climatology in CMIP5/CMIP6 models: Persistent biases and improvements. Revista Facultad de Ingeniería (100): 75-96. https://doi.org/10.17533/udea.redin.20210525

Arias PA, Rendón ML, Martínez JA, Allan RP. 2023. Changes in atmospheric moisture transport over tropical South America: An analysis under a climate change scenario. Climate Dynamics 61: 4949-4969. https://doi.org/10.1007/s00382-023-06833-4

Ashfaq M, Cavazos T, Reboita MS, Torres-Alavez JA, Im E-S, Olusegun CF, Alves L, Key K, Adeniyi MO, Tall M, Sylla MB, Mehmood S, Zafar Q, Das S, Diallo I, Coppola E, Giorgi F. 2021. Robust late twenty-first century shift in the regional monsoons in RegCM-CORDEX simulations. Climate Dynamics 57: 1463-1488. https://doi.org/10.1007/s00382-020-05306-2

Barichivich J, Gloor E, Peylin P, Brienen RJW, Schöngart J, Espinoza JC, Pattnayak KC. 2018. Recent intensification of Amazon flooding extremes driven by strengthened Walker circulation. Science Advances 4. https://doi.org/10.1126/sciadv.aat8785

Bentsen M, Bethke I, Debernard JB, Iversen T, Kirkevåg A, Seland Ø, Drange H, Roelandt C, Seierstad IA, Hoose C, Kristjánsson JE. 2013. The Norwegian Earth System Model, NorESM1-M – Part 1: Description and basic evaluation of the physical climate. Geoscientific Model Development 6: 687-720. https://doi.org/10.5194/gmd-6-687-2013

Bovolo CI, Wagner T, Parkin G, Hein-Griggs D, Pereira R, Jones, R. 2018. The Guiana Shield rainforests-overlooked guardians of South American climate. Environmental Research Letters 13: 074029. https://doi.org/10.1088/1748-9326/aacf60

Brêda JPLF, de Paiva RCD, Collischon W, Bravo JM, Siqueira VA, Steinke EB. 2020. Climate change impacts on South American water balance from a continental-scale hydrological model driven by CMIP5 projections. Climatic Change 159: 503-522. https://doi.org/10.1007/s10584-020-02667-9

Builes-Jaramillo A, Poveda G. 2018. Conjoint analysis of surface and atmospheric water balances in the Andes-Amazon system. Water Resources Research 54: 3472-3489. https://doi.org/10.1029/2017WR021338

Builes-Jaramillo A, Pántano V. 2021. Comparison of spatial and temporal performance of two Regional Climate Models in the Amazon and La Plata river basins. Atmospheric Research 250: 105413. https://doi.org/10.1016/j.atmosres.2020.105413

Builes-Jaramillo A, Yepes J, Salas HD. 2022. The Orinoco Low-Level Jet and its association with the hydroclimatology of northern South America. Journal of Hydrometeorology 23: 209-223. https://doi.org/10.1175/JHM-D-21-0073.1

Buytaert W, Célleri R, De Bièvre B, Cisneros F, Wyseure G, Deckers J, Hofstede R. 2006. Human impact on the hydrology of the Andean páramos. Earth-Science Reviews 79: 53-72. https://doi.org/10.1016/j.earscirev.2006.06.002

Cavazos T, Luna-Niño R, Cerezo-Mota R, Fuentes-Franco R, Méndez M, Pineda Martínez LF, Valenzuela E. 2020. Climatic trends and regional climate models intercomparison over the CORDEX-CAM (Central America, Caribbean, and Mexico) domain. International Journal of Climatology 40: 1396-1420. https://doi.org/10.1002/joc.6276

Dunne JP, John JG, Adcroft AJ, Griffies SM, Hallberg RW, Shevliakova E, Stouffer RJ, Cooke W, Dunne KA, Harrison MJ, Krasting JP, Malyshev SL, Milly PCD, Phillipps PJ, Sentman LT, Samuels BL, Spelman MJ, Winton M, Wittenberg AT, Zadeh N. 2012. GFDL's ESM2 global coupled climate-carbon earth system models. Part I: Physical formulation and baseline simulation characteristics. Journal of Climate 25: 6646-6665. https://doi.org/10.1175/JCLI-D-11-00560.1

Durán-Quesada AM, Gimeno L, Amador J. 2017. Role of moisture transport for Central American precipitation. Earth System Dynamics 8: 147-161. https://doi.org/10.5194/esd-8-147-2017

Escobar M, Hoyos I, Nieto R, Villegas JC. 2022. The importance of continental evaporation for precipitation in Colombia: A baseline combining observations from stable isotopes and modelling moisture trajectories. Hydrological Processes 36: e14595. https://doi.org/10.1002/hyp.14595

Falloon PD, Betts RA. 2006. The impact of climate change on global river flow in HadGEM1 simulations. Atmospheric Science Letters 7: 62-68. https://doi.org/10.1002/asl.133

Frappart F, Papa F, Santos Da Silva J, Ramillien G, Prigent C, Seyler F, Calmant S. 2012. Surface freshwater storage and dynamics in the Amazon basin during the

2005 exceptional drought. Environmental Research Letters 7: 044010. https://doi.org/10.1088/1748-9326/7/4/044010

Funk C, Peterson P, Landsfeld M, Pedreros D, Verdin J, Shukla S, Husak G, Rowland J, Harrison L, Hoell A, Michaelsen J. 2015. The climate hazards infrared precipitation with stations – A new environmental record for monitoring extremes. Scientific Data 2: 1-21. https://doi.org/10.1038/sdata.2015.66

Giorgetta MA, Jungclaus J, Reick CH, Legutke S, Bader J, Böttinger M, Brovkin V, Crueger T, Esch M, Fieg K, Glushak K, Gayler V, Haak H, Hollweg H-D, Ilyina T, Kinne S, Kornblueh L, Matei D, Mauritsen T, Mikolajewicz U, Mueller W, Notz D, Pithan F, Raddatz T, Rast S, Redler R, Roeckner E, Schmidt H, Schnur R, Segschneider J, Six KD, Stockhause M, Timmreck C, Wegner J, Widmann H, Wieners K-H, Claussen M, Marotzke J, Stevens B. 2013. Climate and carbon cycle changes from 1850 to 2100 in MPI-ESM simulations for the Coupled Model Intercomparison Project phase 5. Journal of Advances in Modeling Earth Systems 5: 572-597. https://doi.org/10.1002/jame.20038

Giorgi F, Coppola E, Solmon F, Mariotti L, Sylla MB, Bi X, Elguindi N, Diro GT, Nair V, Giuliani G, Turuncoglu UU, Cozzini S, Güttler I, O'Brien TA, Tawfik AB, Shalaby A, Zakey AS, Steiner AL, Stordal F, Sloan LC, Brankovic C. 2012. RegCM4: Model description and preliminary tests over multiple CORDEX domains. Climate Research 52: 7-29. https://doi.org/10.3354/cr01018

Giorgi F, Coppola E, Teichmann C, Jacob D. 2021. Editorial for the CORDEX-CORE Experiment I Special Issue. Climate Dynamics 57: 1265-1268. https://doi.org/10.1007/s00382-021-05902-w

Gloor M, Brienen RJW, Galbraith D, Feldpausch TR, Schöngart J, Guyot J-L, Espinoza JC, Lloyd J, Phillips OL. 2013. Intensification of the Amazon hydrological cycle over the last two decades. Geophysical Research Letters 40: 1729-1733. https://doi.org/10.1002/grl.50377

Hagedorn R, Doblas-Reyes FJ, Palmer TN. 2005. The rationale behind the success of multi-model ensembles in seasonal forecasting – I. Basic concept. Tellus, Series A: Dynamic Meteorology and Oceanography 57: 219-233. https://doi.org/10.3402/tellusa.v57i3.14657

Hersbach H, Bell B, Berrisford P, Hirahara S, Horányi A, Muñoz-Sabater J, Nicolas J, Peubey C, Radu R, Schepers D, Simmons A, Soci C, Abdalla S, Abellan X, Balsamo G, Bechtold P, Biavati G, Bidlot J, Bonavita M, de Chiara G, Dahlgren P, Dee D, Diamantakis M, Dragani R, Flemming J, Forbes R, Fuentes M, Geer A, Haimberger L, Healy S, Hogan RJ, Hólm E, Janisková M, Keeley S, Laloyaux P, Lopez P, Lupu C, Radnoti G, de Rosnay P, Rozum I, Vamborg F, Villaume S, Thépaut J. 2020. The ERA5 global reanalysis. Quarterly Journal of the Royal Meteorological Society 146: 1999-2049. https://doi.org/10.1002/qj.3803

Hoyos I, Domínguez F, Cañón-Barriga J, Martínez JA, Nieto R, Gimeno L, Dirmeyer PA. 2018. Moisture origin and transport processes in Colombia, northern South America. Climate Dynamics 50: 971-990. https://doi.org/10.1007/s00382-017-3653-6

HyBAm. 2023. SO-HYBAM Amazon basin water resources observations system. Available at: https://hybam.obs-mip.fr/ (accessed 20 October 2023)

IPCC. 2021a. Atlas. In: Climate change 2021 – The physical science basis: Working Group I contribution to the Sixth Assessment Report of the Intergovernmental Panel on Climate Change. Cambridge University Press: 1927-2058. https://doi.org/10.1017/9781009157896.021

IPCC. 2021b. Climate change information for regional impact and for risk assessment. In: Climate change 2021 – The physical science basis: Working Group I contribution to the Sixth Assessment Report of the Intergovernmental Panel on Climate Change. Cambridge University Press: 1767-1926.

Jacob D, Elizalde A, Haensler A, Hagemann S, Kumar P, Podzun R, Rechid D, Remedio AR, Saeed F, Sieck K, Teichmann C, Wilhelm C. 2012. Assessing the Transferability of the Regional Climate Model REMO to Different COordinated Regional Climate Downscaling EXperiment (CORDEX) Regions. Atmosphere 3: 181-199. https://doi.org/10.3390/atmos3010181

Jiménez-Sánchez G, Markowski PM, Jewtoukoff V, Young GS, Stensrud DJ. 2019. The Orinoco Low-Level Jet: An investigation of its characteristics and evolution using the WRF model. Journal of Geophysical Research: Atmospheres 124: 10696-10711. https://doi.org/10.1029/2019JD030934

Kendall MG. 1975. Rank correlation methods, Charles Griffin, London.

Labar RJ, Douglas M, Murillo J, Mejía JF. 2005. The Llanos Low-Level Jet and its association with Venezuelan convective precipitation. National Weather Center Re-

search Experiences for Undergraduates Final Project. Available at: https://caps.ou.edu/reu/reu05/finalpapers/LaBar-finalpaper.pdf

López R, del Castillo CE, Miller RL, Salisbury J, Wisser D. 2012. Examining organic carbon transport by the Orinoco River using SeaWiFS imagery. Journal of Geophysical Research: Biogeosciences 117: 1-13. https://doi.org/10.1029/2012JG001986

Marengo JA. 2005. Characteristics and spatio-temporal variability of the Amazon River basin water budget. Climate Dynamics 24: 11-22. https://doi.org/10.1007/s00382-004-0461-6

Martens B, Miralles DG, Lievens H, Van Der Schalie R, De Jeu RAM, Fernández-Prieto D, Beck HE, Dorigo WA, Verhoest NEC. 2017. GLEAM v3: Satellite-based land evaporation and root-zone soil moisture. Geoscientific Model Development 10: 1903-1925. https://doi.org/10.5194/gmd-10-1903-2017

Martin GM, Bellouin N, Collins WJ, Culverwell ID, Halloran PR, Hardiman SC, Hinton TJ, Jones CD, McDonald RE, McLaren AJ, O'Connor FM, Roberts MJ, Rodriguez JM, Woodward S, Best MJ, Brooks ME, Brown AR, Butchart N, Dearden C, Derbyshire SH, Dharssi I, Doutriaux-Boucher M, Edwards JM, Falloon PD, Gedney N, Gray LJ, Hewitt HT, Hobson M, Huddleston MR, Hughes J, Ineson S, Ingram WJ, James PM, Johns TC, Johnson CE, Jones A, Jones CP, Joshi MM, Keen AB, Liddicoat S, Lock AP, Maidens A V, Manners JC, Milton SF, Rae JGL, Ridley JK, Sellar A, Senior CA, Totterdell IJ, Verhoef A, Vidale PL, Wiltshire A. 2011. The HadGEM2 family of Met Office Unified Model climate configurations. Geoscientific Model Development 4: 723-757. https://doi.org/10.5194/gmd-4-723-2011

Martínez JA, Arias PA, Junquas C, Espinoza JC, Condom T, Domínguez F, Morales JS. 2022. The Orinoco Low-Level Jet and the cross-equatorial moisture transport over tropical South America: Lessons from seasonal WRF simulations. Journal of Geophysical Research: Atmospheres 127: e2021JD035603. https://doi.org/10.1029/2021JD035603

Martínez JA, Arias PA, Domínguez F, Prein A. 2023. Mesoscale structures in the Orinoco basin during an extreme precipitation event in the tropical Andes. Frontiers in Earth Science 11: 1-20. https://doi.org/10.3389/feart.2023.1307549

Meade RH. 2008. Transcontinental Moving and Storage: The Orinoco and Amazon Rivers Transfer the Andes to the Atlantic. Large Rivers: Geomorphology and Management 45-63. https://doi.org/10.1002/9780470723722.ch4

Miranda PT, de Paiva RCD, de Araújo Gama CH, Brêda JPLF. 2023. River discharge in South America: Agreement and contradictions between recent alteration and projected changes. Revista Brasileira de Recursos Hidricos 28: e18. https://doi.org/10.1590/2318-0331.282320220085

Mora A, Moreau C, Moquet JS, Gallay M, Mahlknecht J, Laraque A. 2020. Hydrological control, fractionation, and fluxes of dissolved rare earth elements in the lower Orinoco River, Venezuela. Applied Geochemistry 112: 104462. https://doi.org/10.1016/j.apgeochem.2019.104462

Nieto R, Gallego D, Trigo R, Ribera P, Gimeno L. 2008. Dynamic identification of moisture sources in the Orinoco basin in equatorial South America. Hydrological Sciences Journal 53: 602-617. https://doi.org/10.1623/hysj.53.3.602

Peixoto JP, Oort A. 1992. Physics of climate. 1st ed. American Institute of Physics, Melville, NY, USA, 559 pp.

Pietikäinen JP, Markkanen T, Sieck K, Jacob D, Korhonen J, Räisänen P, Gao Y, Ahola J, Korhonen H, Laaksonen A, Kaurola J. 2018. The regional climate model REMO (v2015) coupled with the 1-D freshwater lake model FLake (v1): Fenno-Scandinavian climate and lakes. Geoscientific Model Development 11: 1321-1342. https://doi.org/10.5194/gmd-11-1321-2018

Reboita MS, Reale M, da Rocha RP, Giorgi F, Giuliani G, Coppola E, Nino RBL, Llopart M, Torres JA, Cavazos T. 2021. Future changes in the wintertime cyclonic activity over the CORDEX-CORE southern hemisphere domains in a multi-model approach. Climate Dynamics 57: 1533-1549. https://doi.org/10.1007/s00382-020-05317-z

Remedio AR, Teichmann C, Buntemeyer L, Sieck K, Weber T, Rechid D, Hoffmann P, Nam C, Kotova L, Jacob D. 2019. Evaluation of New CORDEX Simulations Using an Updated Köppen-Trewartha Climate Classification. Atmosphere 10: 726. https://doi.org/10.3390/atmos10110726

Rodell M, Houser PR, Jambor U, Gottschalck J, Mitchell K, Meng C-J, Arsenault K, Cosgrove B, Radakovich J, Bosilovich M, Entin JK, Walker JP, Lohmann D, Toll D. 2004. The Global Land Data Assimilation System. Bulletin of the American Meteorological Society 85: 381-394. https://doi.org/10.1175/BAMS-85-3-381

Schneider U, Becker A, Finger P, Meyer-Christoffer A, Ziese M, Rudolf B. 2014. GPCC's new land surface precipitation climatology based on quality-controlled in situ data and its role in quantifying the global water cycle. Theoretical and Applied Climatology 115: 15-40. https://doi.org/10.1007/s00704-013-0860-x

Sen PK. 1968. Estimates of the Regression Coefficient Based on Kendall's Tau. Journal of the American Statistical Association 63: 1379-1389. https://doi.org/10.1080/01621459.1968.10480934

Silva León G. 2005. La cuenca del río Orinoco: Visión hidrográfica y balance hídrico. Revista Geográfica Venezolana 46: 75-108.

Solman SA, Blázquez J. (2019). Multiscale precipitation variability over South America: Analysis of the added value of CORDEX RCM simulations. Climate Dynamics 53: 1547-1565. https://doi.org/10.1007/s00382-019-04689-1

Sörensson AA, Ruscica RC. 2018. Intercomparison and uncertainty assessment of nine evapotranspiration estimates over South America. Water Resources Research 54: 2891-2908. https://doi.org/10.1002/2017WR021682

Sorí R, Gimeno-Sotelo L, Nieto R, Liberato MLR, Stojanovic M, Pérez-Alarcón A, Fernández-Álvarez JC, Gimeno L. 2023. Oceanic and terrestrial origin of precipitation over 50 major world river basins: Implications for the occurrence of drought. Science of The Total Environment 859: 160288. https://doi.org/10.1016/j.scitotenv.2022.160288

Sun Q, Miao C, Hanel M, Borthwick AGL, Duan Q, Ji D, Li H. 2019. Global heat stress on health, wildfires, and agricultural crops under different levels of climate warming. Environment International 128: 125-136. https://doi.org/10.1016/j.envint.2019.04.025

Teutschbein C, Seibert J. 2012. Bias correction of regional climate model simulations for hydrological climate-change impact studies: Review and evaluation of different methods. Journal of Hydrology 456-457: 12-29. https://doi.org/10.1016/j.jhydrol.2012.05.052

Urrea V, Ochoa A, Mesa O. 2019. Seasonality of rainfall in Colombia. Water Resources Research 55: 4149-4162. https://doi.org/10.1029/2018WR023316

Valencia S, Marín DE, Gómez D, Hoyos N, Salazar JF, Villegas JC. 2023. Spatio-temporal assessment of Gridded precipitation products across topographic and climatic gradients in Colombia. Atmospheric Research 285: 106643. https://doi.org/10.1016/j.atmosres.2023.106643

Viloria JA, Olivares BO, García P, Paredes-Trejo F, Rosales A. 2023. Mapping projected variations of temperature and precipitation due to climate change in Venezuela. Hydrology 10: 96. https://doi.org/10.3390/hydrology10040096

Wang H, Fu R. 2002. Cross-equatorial flow and seasonal cycle of precipitation over South America. Journal of Climate 15: 1591-1608. https://doi.org/10.1175/1520-0442(2002)015<1591:CEFASC>2.0.CO;2

Warne AG, Meade RH, White WA, Guevara EH, Gibeaut J, Smyth RC, Aslan A, Tremblay T. 2002. Regional controls on geomorphology, hydrology, and ecosystem integrity in the Orinoco Delta, Venezuela. Geomorphology 44: 273-307. https://doi.org/10.1016/S0169-555X(01)00179-9

Watterson IG, Bathols J, Heady C. 2014. What influences the skill of climate models over the continents? Bulletin of the American Meteorological Society 95: 689-700. https://doi.org/10.1175/BAMS-D-12-00136.1

Zhang L, Potter N, Hickel K, Zhang Y, Shao Q. 2008. Water balance modeling over variable time scales based on the Budyko framework. Model development and testing. Journal of Hydrology 360: 117-131. https://doi.org/10.1016/j.jhydrol.2008.07.021